664510

DP-905

AEC RESEARCH AND DEVELOPMENT REPORT

HEAVY WATER MODERATED POWER REACTORS

PROGRESS REPORT
MARCH-APRIL 1964

Technical Division
Wilmington, Delaware

DUPONT
REG. U.S. PAT. OFF.

ISSUED BY

Savannah River Laboratory

Aiken, South Carolina

Printed in USA. Price $1.00
Available from the Office of Technical Services
U. S. Department of Commerce
Washington 25, D. C.

66451 0

DP-905

Reactor Technology
(TID-4500, 29th Ed.)

HEAVY WATER MODERATED POWER REACTORS PROGRESS REPORT MARCH - APRIL 1964

D. F. Babcock, Coordinator
Power Reactor Studies
Wilmington, Delaware

Compiled by R. R. Hood

Issue Date: May 1964

E. I. DU PONT DE NEMOURS & COMPANY
EXPLOSIVES DEPARTMENT - ATOMIC ENERGY DIVISION
TECHNICAL DIVISION - WILMINGTON, DELAWARE

CONTRACT AT (07-2) - 1 WITH THE
UNITED STATES ATOMIC ENERGY COMMISSION

ABSTRACT

Various mechanical problems prevented nuclear operation of the Heavy Water Components Test Reactor (HWCTR) during March and April 1964. Fabrication development was initiated on a set of uranium oxide driver tubes for the HWCTR. These tubes will operate at conditions of interest for D_2O-cooled power reactors and will increase substantially the utilization of the HWCTR as a fuel test reactor. A series of physics experiments on D_2O-moderated mixed lattices was conducted as a test of calculational methods. An equation for prediction of heat transfer burnout for flow of subcooled water in annuli was developed on the basis of 193 burnout experiments. A preliminary analysis indicates that it is technically feasible to substitute liquid H_2O for liquid D_2O coolant in D_2O-moderated power reactors, but the economic gain may be marginal.

CONTENTS

LIST OF TABLES

LIST OF FIGURES

HEAVY WATER MODERATED POWER REACTORS
PROGRESS REPORT
MARCH - APRIL 1964

INTRODUCTION

This report reviews the progress of the Du Pont development program on heavy-water-moderated power reactors. The goal of the program is to advance the technology of these reactors so that they could be used in large power stations to generate electricity at fully competitive costs. Program emphasis is being placed on reactors that are cooled by liquid D_2O. The principal phases of the program are: (1) the irradiation of candidate fuels and other reactor components in the Heavy Water Components Test Reactor (HWCTR), (2) the development of low-cost fuel tubes for use in large water-cooled reactors, and (3) the technical and economic evaluation of various reactor design concepts.

SUMMARY

A series of mechanial problems precluded nuclear operation of the HWCTR during this report period. Debris that was introduced accidentally into the main D_2O system by disintegration of a plywood line plug was removed, and moderator quality was restored to normal by deionization and filtration. Resumption of reactor operation was delayed by failure of (1) four Zircaloy guide tubes for safety rods, (2) mechanical seals on the D_2O pumps in the liquid D_2O loop, and (3) anchor bolts for the gas baffle in the neck of the reactor vessel.

Fabrication development was initiated on a set of uranium oxide driver tubes for the HWCTR. The use of these tubes, which will be irradiated at conditions contemplated for UO_2 tubes in full-scale D_2O-cooled power reactors, will increase substantially the utilization of the HWCTR as a fuel test facility.

Further examinations were made of UO_2 tubes that were irradiated in the HWCTR to a maximum exposure of 9350 MWD/MTU at a peak $\int kd\theta$ of 25 watts/cm. The core appearance and fission gas release in these tubes were consistent with earlier observations on other UO_2 tubes. Examinations were started on two assemblies of UO_2 tubes that failed at low exposures and relatively high thermal ratings (1700 MWD/MTU at $\int kd\theta$ of 56 watts/cm and 1120 MWD/MTU at 68 watts/cm). Sheath failures were discovered in one tube from each assembly; the causes of the failures have not been identified yet. Part of the UO_2 in the assembly that operated at 68 watts/cm melted during irradiation.

A series of experiments on D_2O-moderated mixed lattices was conducted in the Process Development Pile (PDP); the objective was to obtain data for a test of existing calculational methods for predicting the physics parameters of such lattices. Good superficial agreement was obtained between the experimental results and the calculations, but a detailed examination of the results and a comparison with other data cast doubt on the significance of the agreement. Attempts are being made to modify the calculational methods to improve the agreement in detail.

An empirical equation was developed for the prediction of heat transfer burnout for forced flow of subcooled water in annuli. The equation fits the results of 193 burnout tests with a standard deviation of 9%; maximum deviations of the data are +26 and -23%. The equation applies for system pressures of 25 to 1200 psia, water velocities of 5 to 42 ft/sec, and subcoolings of 10 to 95°C (18 to 171°F).

A preliminary investigation was made of the feasibility of using liquid H_2O coolant in a D_2O-moderated power reactor. The results indicate that H_2O coolant is technically feasible, but that the economic gain is marginal if D_2O losses in a D_2O-cooled reactor can be held to 2 to 3%/yr of the inventory. The major difficulty with H_2O coolant is the positive coolant coefficient of reactivity and the attendant problems of reactor stability and control. It appears possible by proper design of the fuel assembly (nested UO_2 tubes) to reduce the power coefficient of reactivity with H_2O coolant to zero or to a small negative value.

DISCUSSION

I. THE HEAVY WATER COMPONENTS TEST REACTOR (HWCTR)

The HWCTR is a D_2O-cooled-and-moderated test reactor in which candidate fuel assemblies and other reactor components are being evaluated under conditions that are representative of large D_2O-moderated power reactors. Currently, fuel assemblies of uranium metal (coextruded with Zircaloy cladding) and assemblies of uranium oxide (mechanically compacted in Zircaloy sheaths) are in this reactor for irradiation testing.

A. REACTOR OPERATION

Various mechanical abnormalities prevented nuclear operation of the reactor during March and April.

The pieces of the plywood line plug that disintegrated in the main D_2O coolant system (see DP-895) were removed manually from the screens above each fuel assembly and from the top face of the horizontal shield. All of the debris was removed, as evidenced by the fact that collection on the screens gradually decreased and finally ceased. The soluble and finely divided contamination from the plywood and masonite parts of the line plug was removed in the moderator purification system. The heavy water was pumped through a D-OD ion exchange resin rather than the usual Li-OD resin, and then through a filter. The turbidity, color, and organic content of the D_2O were returned to normal in two to three days. Lithium hydroxide was added to the effluent from the purification system to adjust the pD to the normal operating range of 10-11 before the D_2O was returned to the reactor.

During a program of heating the heavy water in the reactor system to 200°C with pump heat, one or both mechanical seals on the shafts of the circulating pumps in the liquid-cooled isolated loop opened and released enough D_2O to overflow the seal leak collection system. The reactor was rapidly cooled and depressurized, and the D_2O escape was limited to 2000 pounds. About 1500 pounds of D_2O was recovered from the building sump at 90% purity. Detailed examination of the seals and the seal supply system did not reveal definitely the cause of the seal leakage. The seals were in the closed position when removed from the pumps and were in good mechanical condition. The most likely cause of the failure was a malfunction in the D_2O supply system to the seal cavity. This system was overhauled and is now functioning properly; measures are being taken to decrease the possibility of seal supply malfunction.

During tests of the safety rod drop times, one rod dropped excessively fast and was not hydraulically decelerated at the bottom of its fall. An examination in the reactor revealed that the Zircaloy guide tube for the safety rod was broken near the point where the guide tube is reduced in diameter to produce hydraulic deceleration of the rod (see Figure 1). Subsequent examination also revealed a longitudinal split about 30 inches long beginning in the region of diameter reduction and running toward the bottom of the guide tube (see Figure 2). Splits or cracks were also discovered in three of the other five guide tubes; the remaining two appeared to be undamaged. All of the guide tubes were replaced. The tubes removed from the reactor are being examined in detail to obtain the data required for a new guide tube design.

In the course of these inspections of the interior of the reactor vessel, it was observed that two bolts in the legs that support the gas baffle were completely severed. The bolt heads were found on top of the horizontal shield and were removed. The bolts are 17-4 PH steel in the H1100 condition. The cause of bolt failure cannot be determined with assurance, but examinations indicate that they failed from overextension rather than fatigue, and that the failures occurred some time ago. The support structure for the gas baffle was removed and replaced with one of increased strength and rigidity. Bolts of "Inconel" X* were used to fasten the new support structure because of their greater tensile strength and fatigue resistance as compared to 17-4 PH steel.

B. POSTIRRADIATION EXAMINATION OF DRIVER FUEL TUBES

1. Tubes from First Driver Cycle

Postirradiation examinations of two U-Zr driver fuel tubes from the first HWCTR driver cycle showed good dimensional stability of the drivers under conditions existing in that cycle. The tubes were utilized in the reactor from initial startup (October 1962) until November 1963, at which time driver reactivity became too low to maintain desired irradiation conditions in test fuel assemblies; they were then replaced by a second set of drivers. These two particular tubes were selected on the basis of their exposures and operating temperatures, which were the highest of the 24 tubes in the first charge. Both were inspected on previous occasions, and the inspection described herein completed the history of their dimensional behavior during operation.

The driver tubes contain fuel cores of U^{235} (93% enrichment) alloyed with zirconium; the total uranium concentration is 9.3 wt %. The tubes were fabricated by coextrusion in

*"Inconel" is a trademark of International Nickel Co.

Zircaloy-2 sheaths. Driver fuel tube No. 22 was irradiated to a maximum fission burnup of 1.89 atom % at a time-averaged maximum metal temperature of 498°C. The outside diameter of the tube decreased 14 mils (0.6%) over a section 18 to 33 inches from the top and increased about 5 mils (0.2%) over a section 60 to 78 inches from the top. Maximum cladding strain, calculated on the basis of the maximum increase in outside diameter, was 0.17%. The inside diameter decreased an average of about 8 mils (0.4%). The maximum volume increase was 3.6%. The changes in the OD, ID, and volume are plotted implicitly as functions of exposure in Figure 3.

Driver fuel tube No. 48 was irradiated to a maximum fission burnup of 1.80 atom % at a time-averaged maximum metal temperature of 485°C. Changes in the outside diameter of the fuel tube varied from a 0.7% decrease to a 0.3% increase. The maximum cladding strain calculated on the basis of the maximum increase in outside diameter was 0.28%. The maximum volume increase was 5.0%. Inspection data for this tube are presented in Figure 4.

The final dimensional and volume changes over most of the length of both fuel tubes closely parallel those observed in the earlier examinations. Exceptions are the comparatively large decreases in volume at the top of tube No. 22 and at both ends of tube No. 48. The maximum volume increases were much less than were predicted for fuel of this composition under the stated conditions of burnup and temperature.

2. Tubes from Second Driver Cycle

The second set of HWCTR driver assemblies are of the same design as those of the first set, but have operated at higher metal temperatures (540°C vs. ~500°C maximum). Two tubes from the second set were removed from the reactor for examination after irradiation to a maximum fission burnup of 0.34 atom %. Average dimensional changes were as follows:

Fuel Tube No.	1	18
Change in OD	0.2% decrease	0.2% decrease
Change in ID	0.1% increase	<0.1% increase
Change in volume	1.8% decrease	1.2% decrease

On the basis of these results and postirradiation data from the first driver set, a decision was made to increase the operating temperature of the drivers to a maximum of 580°C. The objective is to increase specific powers in test fuel assemblies in the HWCTR. Further interim examinations will be made to observe dimensional changes in the drivers at the higher temperature.

II. REACTOR PHYSICS

A. FLUX DEPRESSION IN HWCTR BAYONET

It was reported in DP-865 that a structural failure occurred in the Zircaloy-2 bayonet of the HWCTR boiling D_2O loop, and that it was necessary to remove the bayonet from the reactor. In order to increase the strength and to decrease the cost of a replacement bayonet, stainless steel was specified as the material of construction. To provide data for design of the stainless steel bayonet, measurements were made in the Subcritical Experiment (SE) of the neutron flux levels and cadmium ratios in the bayonet as functions of its wall thickness. Although the stainless steel will depress the neutron flux inside the bayonet, the measurements show that the flux will be high enough for meaningful tests of fuel elements at conditions representative of those expected in power reactors. Accordingly, design is proceeding with stainless steel as the material of construction. The SE measurements are described below.

In the performance of the experiments, the SE was loaded uniformly on a 7-inch triangular lattice pitch with the slightly enriched uranium tubes shown in Figure 5. The lattice arrangement is illustrated in Figure 6, which also identifies the test assembly (No. 1) and the two reference positions (Nos. 2 and 3). The fuel at these three positions was machined to accept bare copper foils and cadmium-covered copper foils. The moderator purity was 99.5 mol % D_2O.

Fuel irradiations were made with the central fuel tube bare, with it housed in an aluminum tube (5.000-inch OD x 0.250-inch wall), and with it housed in type 316 stainless steel tubes (5.563-inch OD x 0.258-inch, 0.500-inch, and 0.750-inch walls). The aluminum housing tube provided a mockup of the zirconium housing used in the original bayonet design, while the stainless steel tubes covered the range of possible design thicknesses. Table I lists the thermal flux ratios observed for the test and reference positions under the various test conditions. These data are also plotted in Figure 7. They are corrected for the over-all flux distribution in the SE. Table II illustrates the flux-hardening effect of the stainless steel tubes in terms of the measured cadmium ratios at each of the three measurement positions. The differences between cadmium ratios at the three positions are plotted in Figure 8 as functions of the wall thickness of the stainless steel tubes. These data are in good accord with independent calculations.

B. BUCKLINGS OF MIXED LATTICES

It is anticipated that many power reactors will ultimately operate with mixed lattices, i.e., with lattices that contain two or more different types of fuel assemblies. This situation could arise, for instance, when part of the fuel is recycled or when isotope production is combined with power production. Calculational methods exist which treat such situations, but very little experimental information has been available to test these methods in D_2O-moderated lattices. The following paragraphs discuss a series of mixed lattice experiments that were conducted in the Process Development Pile (PDP) with the objective of providing the required data.

The lattice components in the PDP experiments were limited to available items of simple design, such as single rods or tubes, while the lattices themselves were chosen for convenience of predicted critical moderator height. Each lattice contained 85 elements at a 7.00-inch triangular lattice pitch; with one exception, the lattices were surrounded by a boundary of 36 poison rods. The lattice components are shown in Figure 9, and the lattice patterns are shown in Figure 10.

The experimental measurements determined the vertical and radial bucklings and the neutron density ratios among the different lattice components. Vertical flux traverses to determine the vertical extrapolation distances were obtained by irradiating gold pins. To obtain the vertical buckling, these extrapolation distances were applied to the critical moderator heights measured with the gold removed. A small correction was made to this buckling to account for the presence of aluminum guide tubes for control rods. Radial bucklings were derived from the extrapolated lattice radius, as indicated by the irradiation of copper foils in similar types of rods throughout the lattice or by the irradiation of gold pins in the centers of similar types of tubes. Neutron density ratios among the different lattice components were obtained by irradiating copper foils which had been machined to the same dimensions as the various lattice components. Cadmium-covered copper foils were placed at a different level to allow the epicadmium activity to be subtracted from the bare foil activity in these measurements. A correction for the radial flux shape in the pile yielded the ratios of thermal fluxes averaged over the different lattice components in a flat radial flux. Thermal absorption ratios were derived from these measured neutron densities. The moderator purity was 99.58 mol % D_2O, and the moderator temperature was 19°C for the series of experiments.

Results of the measurements are presented in Table III. Unless one considers the poison ring in Lattice 2 to meet the

requirement, Lattices 1 and 2 are not mixed lattices. These one-component lattices were included to provide an initial test of the calculations without the complications of mixed lattices. Lattice 3 is, however, a mixed lattice with a 3:1 ratio between components; Lattice 4 has a 2:1 ratio and Lattice 5 a 1:1:1 ratio. In addition to the pattern shown in Figure 10, Lattice 5 was rearranged to form the same pattern centered on a fuel rod rather than on a fuel tube. Each lattice was surrounded by moderator extending to the wall of the PDP tank, which has a radius of 247 cm.

In order to establish the precision of the thermal neutron density ratios, two additional flux ratio measurements were made with Lattice 5. These measurements, yielding more scatter in the results than one would expect, indicated that an uncertainty of ±2% should be assigned to a single measurement of flux ratio. The vertical and radial buckling results should have an accuracy of about ±4 μB.

Two different calculational techniques were applied to the analysis of these experiments. One of the techniques is based on the source-sink methods as encoded in HERESY.[1] The other is based on the more conventional multigroup diffusion theory methods as encoded in PDQ-3 code.[2] Both of these codes require extensive input calculations, primarily to compute the fuel assembly absorption parameters (γ for HERESY and Σ_a for PDQ-3). These input parameters were obtained from the THERMOS[3] and BSQ[4] codes. A comparison between the experimental numbers and the HERESY and BSQ results is shown in Table III. A detailed examination of the calculations and a comparison with other heterogeneous lattices investigated at Savannah River cast some doubt on the significance of the good agreement shown in the table. The difficulties seem to be primarily in the THERMOS-BSQ input calculations. A somewhat laborious method for improving the calculations was devised on the basis of iterations between the THERMOS and PDQ calculations. In the iterative calculations, the results of the first PDQ run is used to assign areas of the moderator to be associated with each of the lattice components. A new THERMOS calculation is then made on the basis of these moderator areas, and the results are again substituted into the PDQ code, etc. Two iterations appear to give satisfactory convergence. An attempt is being made to develop a faster substitute for the iterative procedure.

III. REACTOR FUELS

A. GENERAL

Two types of Zircaloy-clad fuel elements are under development in the Du Pont program on D_2O-cooled power reactors: mechanically compacted tubes of uranium oxide, and coextruded tubes of uranium metal. In the development of these two fuels, primary attention is being given to fuel element designs and fabrication methods that offer promise of low fabrication costs when the elements are produced in the volume required for several full-scale reactors. At present, the uranium oxide tubes are receiving program emphasis pending the outcome of current irradiations of both types of fuel in the HWCTR.

In addition to the program on uranium fuels, a modest irradiation program has been initiated on thorium fuels (see DP-885). The ultimate objective of this program is to develop fuel elements that would be suitable for use in D_2O-thorium breeder reactors.

B. URANIUM OXIDE TUBES

1. Fabrication of Irradiation Specimens

Fabrication started on short irradiation specimens of a large oxide tube (3.7-inch OD) that is similar in size to the outer fuel tube in the three-tube assembly described in DP-830.[5] This is the largest tube on which a fabrication attempt has been made thus far. Seven test pieces, each about 1 ft long, will be assembled into a fuel column for irradiation in the HWCTR at thermal ratings ($\int kd\theta$) as high as 30 watts/cm and exposures as high as 30,000 MWD/MTU. One column for flow testing has been completed, and two columns for irradiation will be completed in May (assemblies SOT-8-2, SOT-8-3). The irradiation specimens contain fused and crushed UO_2 cores compacted by vibration-plus-swaging to greater than 90% of theoretical density. The UO_2 in the irradiation specimens was enriched to 1.2% U^{235} by mechanically blending natural UO_2 and 1.5% enriched UO_2.

2. Electron Beam Welding Facility

An electron beam welding facility is being installed at the Savannah River Laboratory to develop welding techniques for attaching spacer ribs to the Zircaloy cladding of power reactor fuel tubes. Initial tests at Dresser Products, Inc., indicated that electron beam welding is a feasible method of attaching spacer ribs to fuel or housing tubes (DP-845, DP-855). The new facility contains a high-voltage welder (150 kv - 6 kw

rating) modified to accept 16-inch-diameter, 16-ft-long extensions to each end of the vacuum chamber. A feeding mechanism will move tubes (up to 15-1/4 ft long) beneath the electron beam; accurate positioning of the tube is obtained by a separate guidance system. The tube can be rotated or indexed while in the chamber extension to make circumferential welds or to attach several longitudinal spacing ribs with a single pumpdown cycle. Design of the facility is complete, and the welding machine is installed and operating. The chamber extensions, drive mechanism, and guidance system will be installed in May.

3. Oxide Driver Tubes for the HWCTR

At present, 24 of the 36 fuel lattice positions of the HWCTR are occupied by driver fuel assemblies that contain fuel cores of uranium-zirconium alloy (9.3 wt % U). Since core compositions of this type are not being considered for use in D_2O-moderated power reactors, the irradiation experience being obtained with the drivers contributes little to the program. To overcome this disadvantage, and thereby to increase greatly the effective utilization of the HWCTR as a fuel test facility, plans are being made to produce driver tubes of uranium oxide and use them in the reactor as soon as possible. The conceptual design of the oxide driver assembly specifies two nested tubes of mechanically compacted UO_2 (45% U^{235}) in Zircaloy-2 sheaths. Fabrication techniques and irradiation conditions will be those of direct interest for D_2O-cooled power reactors.

~ 4%

As the first step in adapting mechanical compaction techniques to the oxide drivers, loading tests were begun on a mockup of the outer oxide tube. These tests are aimed at developing techniques required to load this size element to at least 82% of theoretical density with a maximum core thickness variation of ±5%. The mockup element is 9 ft long; after swaging, the OD and core thickness are expected to be about 2.54 inches and 0.178 inch, respectively. Core densities in the first two loading tests were satisfactory (82 to 82-1/2% of theoretical), but wall thickness variations were excessive (±11 and ±14%). The tubes will be unloaded and then reloaded under different loading conditions (smaller increments of UO_2 charge) to determine the conditions that result in acceptable core densities and thicknesses.

4. Postirradiation Examination of Irradiation Specimens Assembly SOT-1-3

Analyses of gases released from the oxide core during irradiation and postirradiation sectioning were completed on the seven short fuel tubes from the SOT-1-3 assembly. These

fuel pieces were irradiated without incident to a burnup of 9,350 MWD/MTU at a peak thermal rating of 25 watts/cm. The irradiation conditions and pertinent information on the fabrication histories are shown in Table IV; preliminary inspection results were reported in DP-895.

The analyses of the free gas in the tubes after irradiation are listed in Table V. The two elements that operated at the highest power (about 22 watts/cm, time-averaged peak $\int kd\theta$) released 8 to 13% of the total fission-product xenon. The percentage release of xenon varied with thermal rating in a manner consistent with that observed in tubes irradiated previously to lower exposures (DP-875); the data are shown in Figure 11.

The appearance of the UO_2 cores was consistent with that of tubes irradiated earlier at similar thermal ratings. Tube ZE-225E (max. $\int kd\theta$ of 25 watts/cm) exhibited interparticle cohesion and gross cracking of the core, but no evidence of columnar grain growth.

Assembly SOT-5-2

Examination of the fuel pieces from assembly SOT-5-2 is underway. This assembly of seven short UO_2 tubes was discharged from the HWCTR because of a sheath failure after operation to a peak exposure of 1700 MWD/MTU at a maximum thermal rating of 56 watts/cm. The irradiation conditions and fabrication data are shown in Table VI.

A small hole was detected in element Z-259D by pressurizing the core space of the tube with argon, immersing the pressurized tube in water, and searching for bubbles. The hole was in the Zircaloy outer sheath over the UO_2 core, but could not be identified by 20X visual examination. A section of the sheath containing the defect was removed from the tube for further study. A small area of the inner surface of the section exhibits a white deposit, possibly zirconium oxide, in the vicinity of the defect.

Moderate ridging of the outer sheath occurred in one of the two tubes irradiated in assembly SOT-5-2 at the highest rating (51 watts/cm). Tube Z-261D, fabricated with a swaged core of about 89% of theoretical density, ridged slightly but did not fail during irradiation; the ridge was about 7 inches long and increased the diameter of the outer sheath by about 0.034 inch. The element that failed, Z-259D, was fabricated to about the same core density (89-1/2%), and also operated at 51 watts/cm, but did not develop a sheath ridge.

Analyses of the free gas in the SOT-5-2 elements are shown in Table V. The percentage release of fission-product xenon is shown in Figure 11 as a function of the thermal rating of the elements. The xenon release increased linearly with thermal rating from about 25 to 65 watts/cm (the highest rating at which data are available). Also, the release was substantially lower for tubes that contained substoichiometric UO_2 than for tubes with stoichiometric UO_2.

The nitrogen released during irradiation of vacuum-outgassed UO_2 varied from 1 to 12 cc/kg UO_2 (STP) and averaged 8 cc/kg UO_2. This result compares favorably with the behavior of the SOT-1-3 elements, which released 26 to 101 cc/kg UO_2 of nitrogen (average: 65 cc/kg UO_2). The data demonstrate the greater effectiveness of the outgassing conditions that were used in preparing the UO_2 for the SOT-5 elements. The nitrogen released in the three SOT-5-2 elements that contained hydrogen-annealed or substoichiometric UO_2 was extremely low, indicating that alternative ways of controlling the release of sorbed gases from fused UO_2 during irradiation are feasible.

Assembly SOT-7-2

Examination of the fuel pieces from assembly SOT-7-2 is underway. This assembly of seven short UO_2 tubes was discharged from the HWCTR because of a sheath failure after maximum exposure of 1120 MWD/MTU was reached at a maximum thermal rating of 68 watts/cm. The irradiation conditions and fabrication data are listed in Table VII.

A hole was detected in the inner sheath of tube ZE-266A, the hottest tube in the assembly. The hole was about 0.050 inch in diameter and was located over the void chamber near the top of the tube about 0.2 inch above the top end of the core. The nature and cause of the failure are being investigated.

Core sections near the top of this tube revealed that the tube operated with part of the UO_2 molten. A 1-1/2-inch-long annular void in this region apparently resulted from shrinkage of the molten core on solidification (Figure 12). Some of the UO_2 penetrated into the upper void chamber; in the vicinity of the failure, the septum between the core and void space was deformed inward toward the void. The outer sheath of the tube was bulged over most of its lower half. The maximum increase in diameter was about 0.072 inch (3.5%), and the average increase in OD was about 0.040 inch; the core volume increased 4%.

Assembly SOT-7-2 contained six other tubes that operated satisfactorily; core sections from tube ZE-266C indicate that this tube also operated with central melting of the core. Examination of these tubes is in progress.

IV. HEAT TRANSFER BURNOUT IN SUBCOOLED WATER

In DP-725, experimental data were presented on heat transfer burnout for forced flow of subcooled water in tubes and annuli at pressures up to 1000 psia; correlating equations for the data also were presented. Subsequently, additional data were obtained at the Savannah River Laboratory and at Columbia University for flow in annuli. On the basis of the new data, which extend the range of test conditions, a new correlating equation was developed. This equation, which is now being used for calculation of burnout heat fluxes in HWCTR fuel assemblies, is discussed in the following paragraphs.

The results of 193 burnout tests with annular coolant passages were correlated by the following empirical equation:

$$\Phi_{BO} = 257{,}000(1 + 0.040V)(1 + 0.030T_s)$$

The nomenclature and ranges of variables that are correlated by the equation are as follows:

Φ_{BO} = heat flux at burnout, 10^6 pcu/(hr)(ft^2): 0.5 to 2

V = velocity of coolant, ft/sec: 5 to 42

T_s = subcooling, °C: 10 to 95

Pressure, psia: 25 to 1200

Length of heated surface, inches: 19 to 40

Annulus diameter of curvature, inch:
ID, 0.5 to infinity; OD, 0.75 to infinity

Equivalent diameter, inch: 0.25 to 1

Flow of water vertically downward

The experimental data fit this equation with a standard deviation of 9.1%. The maximum deviations are +26.1 and -22.8%.

The burnout data were obtained at Savannah River with a rectangular channel heated on one side and with an annulus that was heated on its inner wall. This equipment is described in Reference 6. The Columbia University experiments were performed on an annulus formed by large-diameter tubes, as described in DP-805. A total of 223 applicable tests were obtained with the three test arrangements. Seven tests were omitted from the correlation because of poor heat balances, and one because of a suspected hot spot. Twenty-two other tests were omitted because the subcooling and velocity were beyond the ranges in which the linear relationships of the correlation are valid.

The burnout heat fluxes in the 22 tests where the subcooling was less than 10°C regardless of velocity, or less than 20°C at velocities below 5 ft/sec, were higher than would be calculated by the new burnout equation. These 22 points are identified in Figures 13 and 14, which show the fit of the equation throughout the ranges of velocity and subcooling. As illustrated in the figures, the correlation is conservative by as much as 45% for the three following combinations of velocity and subcooling: <42 ft/sec, <10°C, <10 ft/sec, <15°C; and <5 ft/sec, <20°C. The mechanism responsible for the departure of the data from the linear relationships at low subcooling and low velocity has not been identified.

The burnout heat flux was not affected by the system pressure. The test results are plotted against pressure in Figure 15. This figure shows no consistent drift of the data from the correlation; the standard deviation of the correlation could not be decreased significantly by including a pressure term in the equation.

The correlating equation of DP-725 is as follows:

$$\Phi_{BO} = 490{,}000(1 + 0.040V)(1 + 0.010T_s)$$

This equation and the new equation are compared in Figure 16 with each other and with the experimental data.

V. REACTOR DESIGN AND EVALUATION STUDIES

One of the disadvantages of using heavy water to cool a power reactor is the cost of the D_2O. The capital cost of the D_2O inventory is an important component of the power generation cost, and extreme care must be taken to limit D_2O losses during reactor operation. For these reasons, light water is of interest as an alternative coolant. There are two situations to consider: (1) design the reactor for the exclusive use of light water, (2) design for heavy water cooling, but employ light water during initial stages of operation to greatly reduce the risk of losing a large amount of D_2O during this period. The following paragraphs discuss a preliminary study of the feasibility of liquid H_2O cooling.

The major difficulty in the use of light water coolant results from the positive coolant coefficient of reactivity and the attendant control and stability problems. A preliminary analysis indicates that it is possible to decrease the positive coolant coefficient sufficiently to make this kind of operation feasible. To reduce the coolant coefficient, the fuel assembly must be designed for low volume of H_2O. With the smaller coolant

passages, the coolant velocity and pressure drop will be correspondingly increased. If H_2O is to be used on an interim basis, sufficient pumping capability must be provided in the original reactor design to accommodate the higher head loss.

The basis for the preliminary study was a D_2O-cooled reactor fueled with nested tubes of UO_2. The fuel assembly design for the D_2O-cooled reactor was modified for H_2O cooling by placing a Zr-clad magnesium filler-rod at the axis of the assembly, thus reducing the coolant volume by about 20%. The fuel assembly dimensions for the D_2O-cooled design and the modified design are listed in Table VIII. To remove the same power, the coolant velocity must be increased from about 45 ft/sec for D_2O to about 60 ft/sec for H_2O. Reactivity coefficient calculations for the modified design are summarized in Table IX, where they are compared with the calculations of the coefficient for H_2O substitution in the original fuel design. These calculations were performed for fuel having the following assay: U^{235}, 0.40%; Pu^{239}, 0.29%; Pu^{241}, 0.025%); and Pu^{240}, 0.10%. This assay corresponds to the composition of fuel in the reactor at the end of a fuel cycle.

The major positive component of the prompt coefficient of reactivity results from the change in the thermal utilization, f, due to the density change of the light water. The major negative component is that related to the Doppler broadening of the U^{238} resonances. The calculations show that the net prompt coefficient is reduced from +22 to +6 x 10^{-5} k/°C of coolant by making the fuel design modification. There are at least three other components of the reactivity coefficient which were neglected; all three are negative. These are (1) the Doppler coefficient associated with the Pu^{240} resonance, (2) the effect of epithermal captures in the fuel, and (3) the effect of reactor leakage in the buckled zone. It is concluded that these factors, in addition to other reasonable modifications of the fuel assembly, will be sufficient to reduce the prompt coefficient to zero or to a slightly negative value.

Replacement of D_2O coolant by H_2O produces cost reductions due to the savings in D_2O inventory and a decrease in D_2O losses. These reductions are offset by cost increases that result from (1) an increase in U^{235} enrichment for the same fuel exposure to compensate for the neutron absorptions in H_2O, and (2) an increase in the cost of pumping because of the higher head loss across the reactor core. Preliminary estimates indicate that if D_2O losses in a D_2O-cooled plant can be limited to 2 to 3%/yr of the inventory, the savings in D_2O cost in an H_2O-cooled reactor are nearly counterbalanced by the higher uranium and pumping costs. Further design and cost evaluations of H_2O cooling will be made so as to obtain a firmer estimate of the relative economics of the two coolants.

TABLE I

Thermal Flux Ratios in Stainless Steel Bayonets

(Data from Subcritical Experiment)

Test Assembly Housing	Φ_1/Φ_2(a)	Φ_1/Φ_3(a)	Φ_1/Φ_2(b)	Φ_1/Φ_3(b)
0.26" stainless steel	0.5792	0.4596	0.5941	0.4872
0.50" stainless steel	0.4044	0.2900	0.4148	0.3074
0.75" stainless steel	0.2863	0.1954	0.2937	0.2071

(a) Normalized to reference run with no housing tube; subscripts refer to position numbers in Figure 6.

(b) Normalized to run with 0.25-inch Al housing; subscripts refer to position numbers in Figure 6.

TABLE II

Cadmium Ratios in Fuel Tubes in SE Experiments

(0.010-inch-thick Cu foils)

Test Assembly Housing	Assembly #1	Assembly #2	Assembly #3
None	12.7	13.1	13.1
0.25" aluminum	12.2	12.5	12.3
0.26" stainless steel	8.4	12.1	12.8
0.50" stainless steel	6.5	11.3	12.9
0.75" stainless steel	5.1	11.5	13.1

Note: See Figure 6 for location of assemblies in lattice.

TABLE III

Comparison of Experimental Bucklings with Predictions of HERESY Code

Lattice[a]	Components[b]	Experiment B_z^2, μB	Experiment B_r^2, μB	Experiment B_m^2, μB	HERESY B_z^2, μB	HERESY B_r^2, μB	HERESY B_m^2, μB
1	III	269	-	-	272	-	-
2	III/V	98	531	629	105	534	639
3	IV/V	97	502	599	78	517	595
4	I/III/V	223	524	747	228	515	743
5 (I centered)	I/II/III/V	341	518	859	380	514	894
5 (III centered)	I/II/III/V	334	-	-	372	523	895

Thermal Neutron Absorption Ratios[c]

Lattice	Assemblies Ratioed	Experiment	HERESY
3	V/IV	1.46 ±0.03	1.45
4	I/III	3.36 ±0.07	3.61
5	I/III	3.28 ±0.05	3.62
	I/II	1.64 ±0.04	1.76
	II/III	2.00 ±0.04	2.06

(a) See Figure 10 for lattice descriptions.
(b) See Figure 9 for component descriptions.
(c) The following values from THERMOS were used to calculate absorption ratios from neutron density (n) ratios.

$$\text{Absorption} = n_{exp} \cdot \frac{\phi}{n} \cdot \Sigma_a \cdot \text{Area}$$

Component	ϕ/n	Σ_a, cm^{-1}
I	1.4463	.24285
II	1.3848	.30678
III	1.2937	.27304
IV	1.2638	.19732
V	1.3387	.51355

TABLE IV

Characteristics and Irradiation Conditions of UO_2 Tubes in Assembly SOT-1-3

Tube No.	Method of Compaction[b]	Core Density, % of Theoretical	$\int kd\theta$, watts/cm: Average in Time and Space	$\int kd\theta$, watts/cm: Time-Averaged Peak	$\int kd\theta$, watts/cm: Maximum Peak	Peak Burnup, MWD/MTU
ZE-232F[a]	V	84.3	4.4	7.5	12.2	3450
ZE-225A	V+S	90.4	11.1	13.6	19.7	6000
ZE-228D	V	84.1	16.8	18.9	22.6	8475
ZE-225E	V+S	90.5	21.0	21.6	25.2	9350
ZE-228G	V	85.5	20.4	20.8	24.5	9350
ZE-222G	V+S	90.6	16.0	18.7	21.8	8175
ZE-228B	V	84.3	9.3	12.6	13.9	5400

(a) All tubes contained stoichiometric UO_2, enriched to 1.5% U^{235}, vacuum outgassed at 1000°C.
(b) V - compacted by vibration only.
V+S - compacted by swaging.

TABLE V

Free Gas in Irradiated UO_2 Tubes

Tube No.	Gas Release (Major Constituents Only), N > cc/kg UO_2 at STP: Total	Xe	N_2	D_2	He	A	Volume of He + A, cc at STP	Initial Free Volume, cc	Xenon Release, % of that Produced by Fission
Assembly SOT-1-3									
ZE-232F	48	0.90	25.5	0	20.1	1.02	47.2	55	1.9
ZE-225A	97	3.14	74	0	15.7	2.98	42.6	41	3.4
ZE-228D	94	5.7	61	0	24.7	1.42	58.2	56	4.0
ZE-225E	135	13.8	101	0	13.6	4.5	43.7	41	8.0
ZE-228G	136	22.2	83	0	26.1	0.15	59.3	53	12.9
ZE-222G	76	7.1	49	0	15.4	3.5	45.2	40	5.2
ZE-228B	93	1.82	66	0	23.8	0.50	54.1	56	2.4
Assembly SOT-5-2									
Z-262A	27.3	0.19	~~11.0~~ 3.0	0	22.6	1.25	96.0	122	2.6
Z-260C	24.9	2.06	~~0.66~~ 0.16	0	21.8	0.49	88.8	99	13.5
Z-259C	39.1	10.6	0.90 0.35	0	22.8	3.68	78.0	101	43.5
Z-259D	Gas lost through hole in sheath							101	
Z-261D	36.9	10.6	0.13 0.05	0	22.5	2.07	96.4	101	34.0
Z-261B	27.1	3.69	~~0.11~~ 0.03	0	22.0	0.97	88.1	102	15.4
Z-262B	28.2	0.37	12.5 3.5	0	23.0	1.18	96.6	123	3.3

TABLE VI

Characteristics and Irradiation Conditions of UO_2 Tubes in Assembly SOT-5-2

Tube No.	Oxide Treatment or Type[a]	Method of Compaction[b]	Core Density, % of Theoretical	∫kdθ, watts/cm: Average in Time and Space	∫kdθ, watts/cm: Time-Averaged Peak	∫kdθ, watts/cm: Maximum Peak	Peak Burnup, MWD/MTU
Z-262A	Vacuum outgassed at 1400°C	V	85.5	12.5	17	31	540
Z-260C	Hydrogen annealed at 1700°C	V+S	89.9	24	30	50	980
Z-259C	Vacuum outgassed at 1400°C	V+S	89.3	39	44	55	1480
Z-259D[c]	Vacuum outgassed at 1400°C	V+S	89.5	50	51	56	1700
Z-261D	Substoichiometric	V+S	89.2	50	51	56	1700
Z-261B	Substoichiometric	V+S	89.1	38	44	48	1460
Z-262B	Vacuum outgassed at 1400°C	V	85.3	18.5	27	28	880

(a) All tubes contain UO_2 of natural enrichment.
(b) V - compacted by vibration only.
V+S - compacted by vibration followed by swaging.
(c) Failed during irradiation.

TABLE VII

Characteristics and Irradiation Conditions of UO_2 Tubes in Assembly SOT-7-2

Tube No.	Oxide Treatment or Type	Core Density, % of Theoretical	∫kdθ, watts/cm: Average in Time and Space	∫kdθ, watts/cm: Time-Averaged Peak	∫kdθ, watts/cm: Maximum Peak	Peak Burnup, MWD/MTU
Z-265C	Vacuum outgassed at 1400°C	90.4[a]	5.7	8	10.8	140
Z-261C	Substoichiometric	89.6	13	16	21	280
Z-260B	Hydrogen annealed at 1700°C	89.2	23	29	40	480
ZE-266C[b]	Vacuum outgassed at 1400°C	88.7	51	58	66	990
ZE-266A[b][c]	Vacuum outgassed at 1400°C	90.8	65	66	68	1120
Z-264A	Hydrogen annealed at 1300°C	89.9	50	52	53	880
Z-265B	Vacuum outgassed at 1400°C	90.3	34	41	42	690

(a) All tubes compacted by vibration plus swaging.
(b) Enriched to 0.9% U^{235} by mechanically blending natural UO_2 with 1.5% enriched UO_2; all other tubes contain UO_2 of natural enrichment.
(c) Failed during irradiation.

TABLE VIII

Fuel Assembly Dimensions
Comparison of D_2O-and H_2O-Cooled Designs

(Dimensions are in inches, unless otherwise noted)

		D_2O Design	H_2O Design
Calandria tube,	OD	4.84	4.84
	ID	4.78	4.78
Pressure tube,	OD	4.66	4.66
	ID	4.22	4.22
Housing tube,	OD	4.10	4.10
	ID	4.04	4.04
Fuel tubes - clad diameters			
No. 1	OD	3.68	3.80
	ID	3.16	3.39
No. 2	OD	2.56	3.01
	ID	1.92	2.45
No. 3	OD	1.28	2.05
	ID	0.61	1.48
Filler rod	OD	-	1.20
Active core length, ft		15	15
Average cladding thickness		0.025	0.025
Coolant area, in^2		6.77	5.66
Coolant-to-fuel area, dimensionless		1.12	0.94

TABLE IX

Reactivity Coefficients of
Fuel Assemblies Cooled with H_2O

	Ref. D_2O Design	Modified Design
f, $k/^oC$	41×10^{-5}	25×10^{-5}
p, $k/^oC$	-5×10^{-5}	-5×10^{-5}
η, $k/^oC$	$+5 \times 10^{-5}$	$+5 \times 10^{-5}$
	41×10^{-5}	25×10^{-5}
Doppler coefficient: $k/^oC$ fuel	-0.95×10^{-5}	-0.95×10^{-5}
ΔT fuel/ΔT coolant	20	20
$k/^oC$ coolant	-19×10^{-5}	-19×10^{-5}
Net $k/^oC$ coolant change	$+22 \times 10^{-5}$	6×10^{-5}

Note: See Table VIII for description of fuel assemblies.

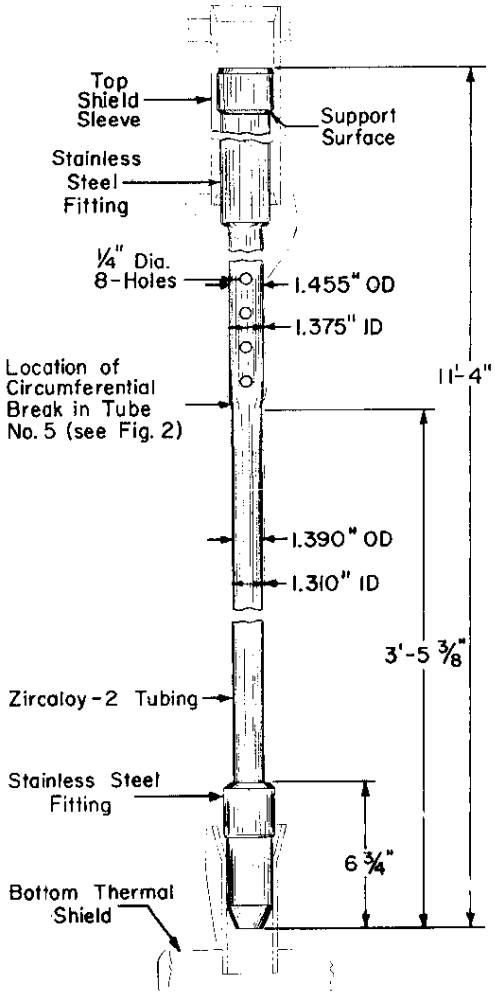

FIG. 1 HWCTR SAFETY ROD GUIDE TUBE

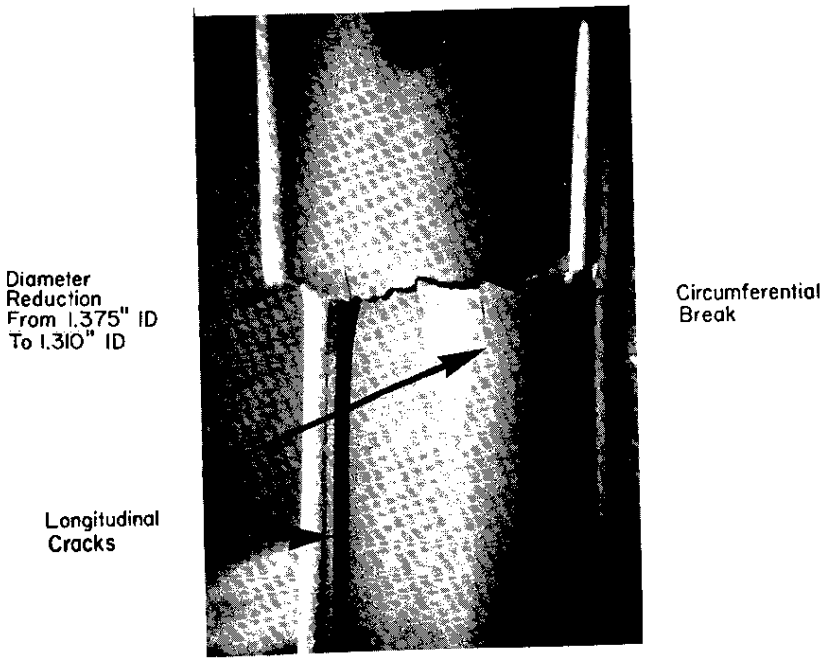

Material: Zircaloy-2, drawn and annealed

FIG. 2 FRACTURES IN SAFETY ROD GUIDE TUBE

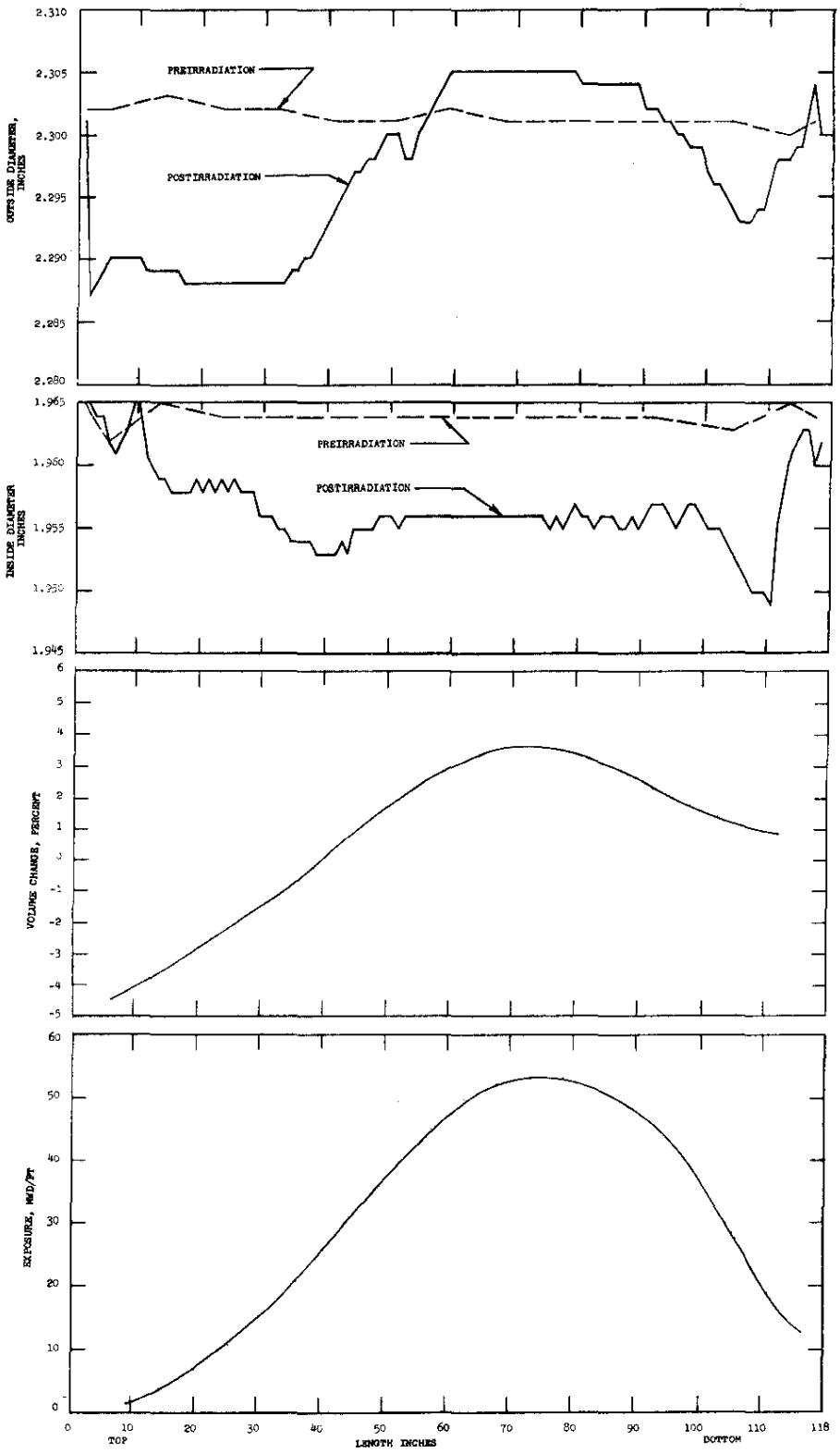

FIG. 3 HWCTR DRIVER ASSEMBLY NO. 15, FUEL TUBE NO. 22

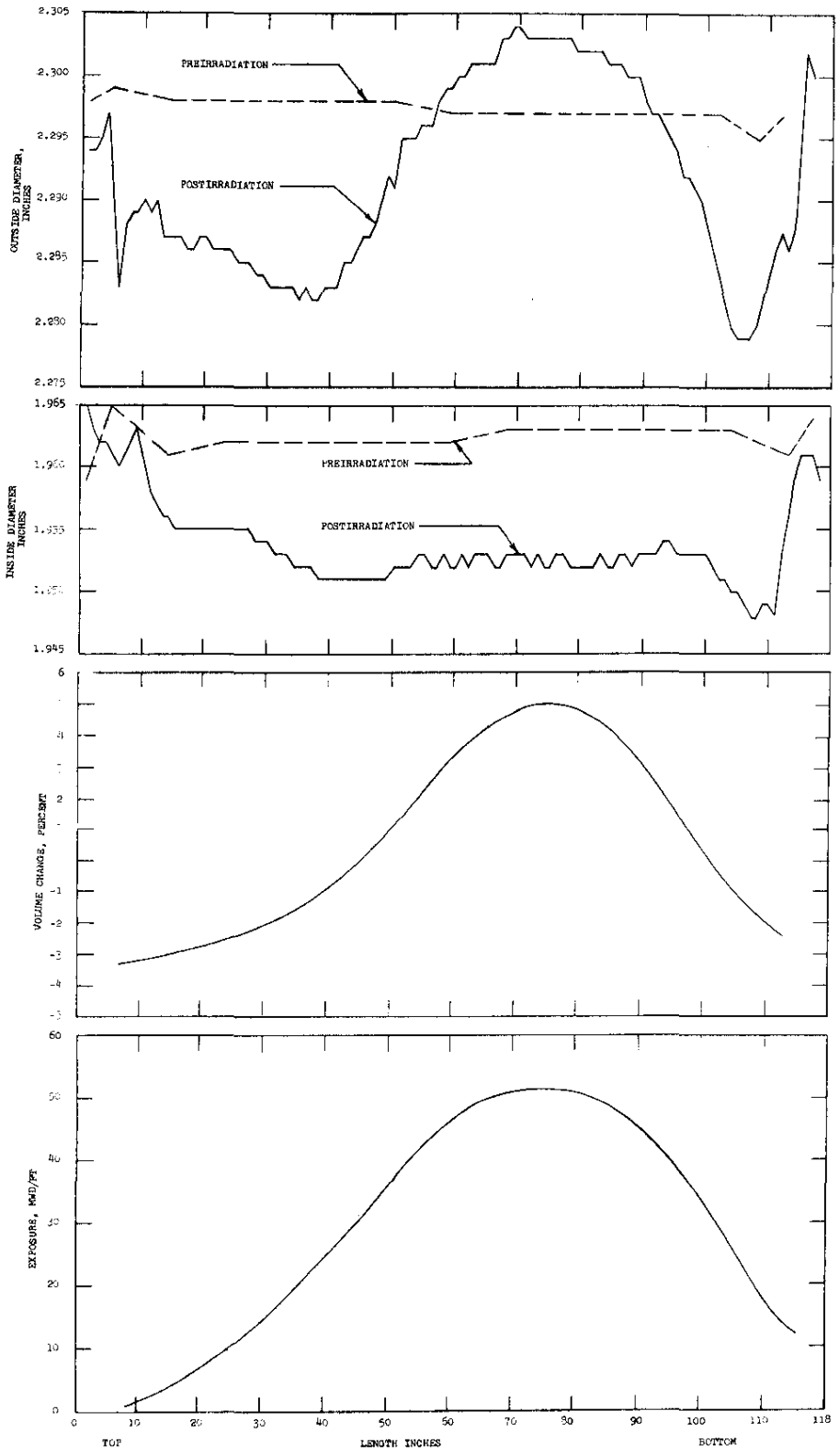

FIG. 4 HWCTR DRIVER ASSEMBLY NO. 11, FUEL TUBE NO. 48

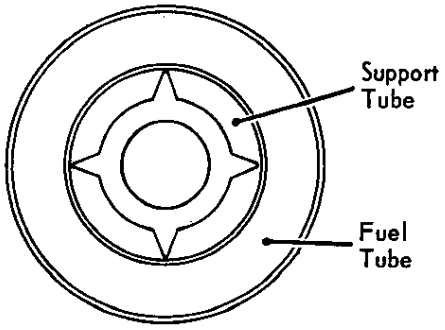

Clad Uranium Metal Tube
Enrichment = 0.947 wt % U^{235}
Density = 18.9 g/cm^3
Cladding and Inner Support Tube
Material = 1100 Aluminum
Clad OD = 1.974 inch
Clad ID = 1.166 inch
Bare Fuel OD = 1.914 inch
Bare Fuel ID = 1.226 inch
Support Tube OD = 0.832 inch
Support Tube ID = 0.532 inch
Support Tube Rib D. = 1.146 inch

FIG. 5 FUEL ASSEMBLY USED FOR SE TESTS OF HWCTR BAYONET

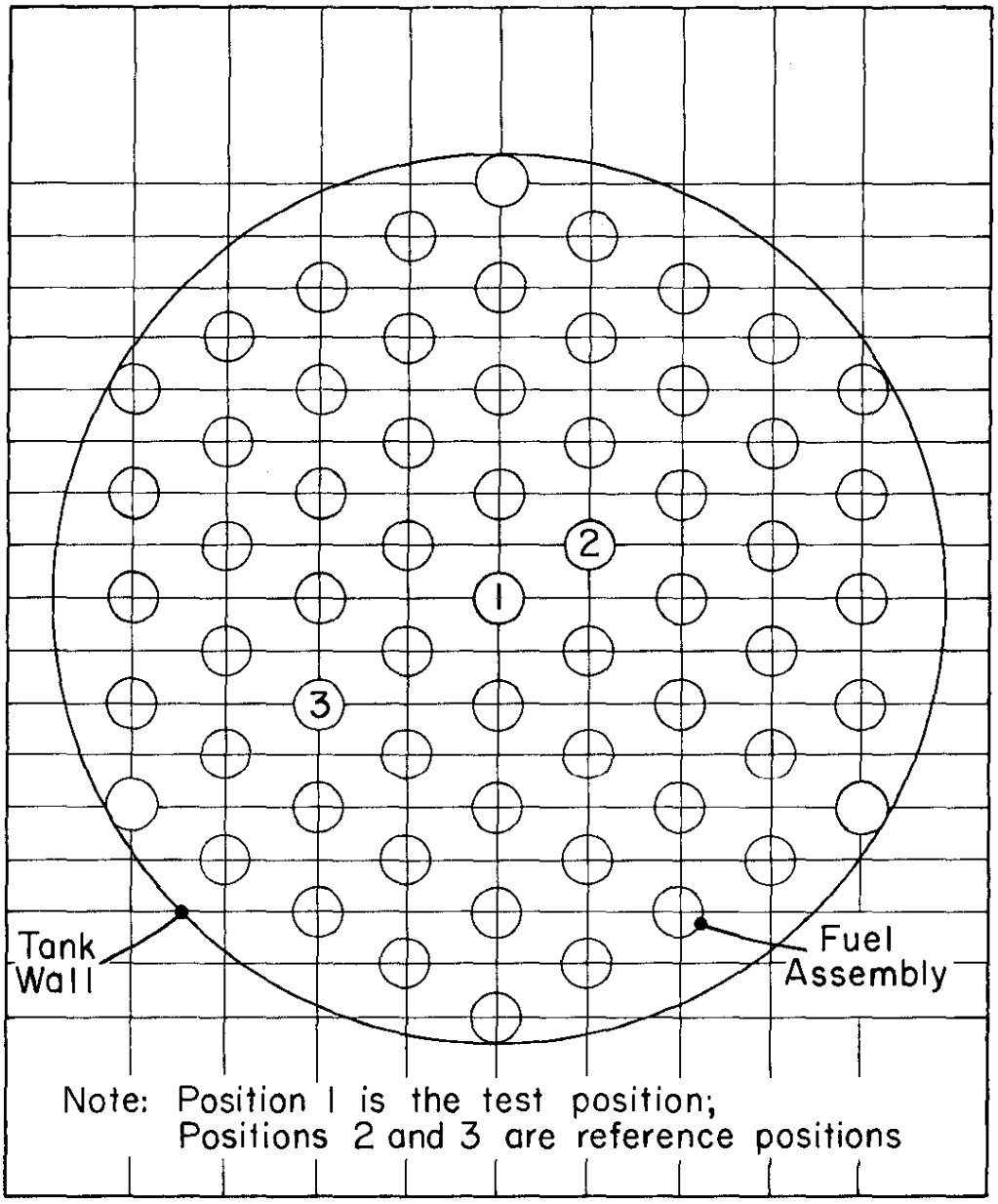

FIG. 6 SE LATTICE DIAGRAM FOR HWCTR BAYONET TESTS

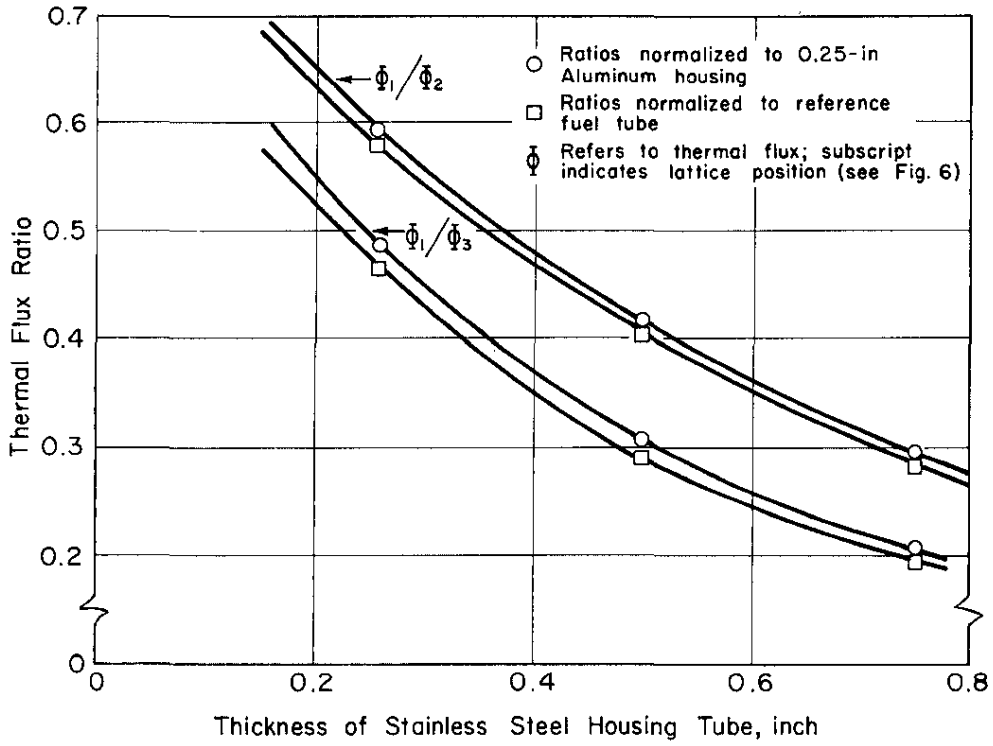

FIG. 7 THERMAL FLUX DEPRESSION IN STAINLESS STEEL BAYONETS

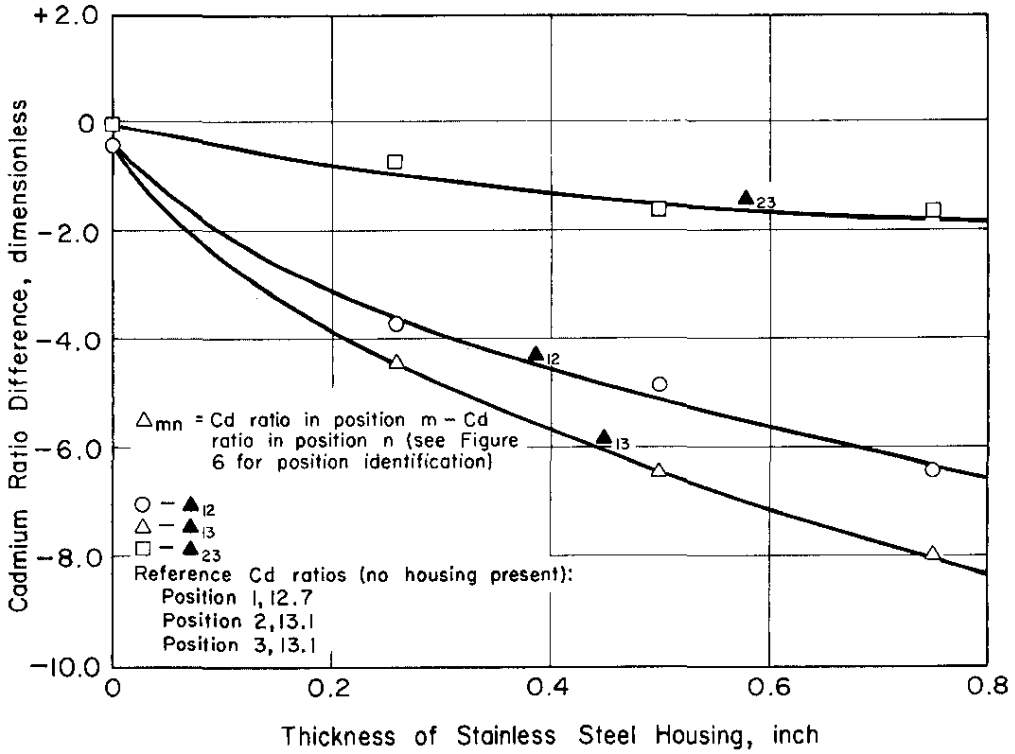

FIG. 8 EFFECT OF STAINLESS STEEL HOUSING THICKNESS ON CADMIUM RATIO DIFFERENCES

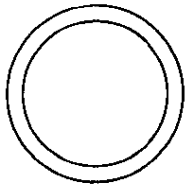

I.
NATURAL URANIUM METAL TUBE
DENSITY = 18.9 gm/cm^3
O.D. = 3.500 inch
I.D. = 2.860 inch

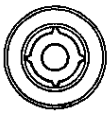

II.
CLAD URANIUM METAL TUBE
ENRICHMENT = 0.947 wt. % U-235
DENSITY = 18.9 gm/cm^3
CLADDING AND INNER SUPPORT TUBE MATERIAL = 1100 ALUMINUM
CLAD O.D. = 1.974 inch
CLAD I.D. = 1.166 inch
BARE FUEL O.D = 1.914 inch
BARE FUEL I.D. = 1.226 inch
SUPPORT TUBE O.D. = 0.832 inch
SUPPORT TUBE I.D = 0.532 inch
SUPPORT TUBE RIB D. = 1.146 inch

III
NATURAL URANIUM METAL ROD
DENSITY = 18.9 gm/cm^3
ROD O.D. = 0.998 inch
SHEATH MATERIAL = 1100 ALUMINUM
SHEATH O.D. = 1.090 inch
SHEATH I.D. = 1.026 inch
AIR BETWEEN SHEATH AND FUEL

IV
ENRICHED URANIUM-ALUM ALLOY ROD
ENRICHMENT > 90 % U-235
5.0 wt % U-235 in ALUMINUM
DENSITY = 2.82 gm/cm^3
ROD O.D. = 1.000 inch
SHEATH MATERIAL = 1100 ALUMINUM
SHEATH O.D. = 1.090 inch
SHEATH I.D. = 1.026 inch
AIR BETWEEN SHEATH AND FUEL

V
NATURAL LITHIUM-ALUM ALLOY ROD
LITHIUM IN ALUMINUM wt % = 4.9
DENSITY OF ALLOY = 2.35 gm/cm^3
ROD O.D. = 0.930 inch
CLADDING & SHEATH MATERIAL = 1100 ALUM.
CLADDING O.D. = 1.005 inch
CLADDING I.D. = 0.930 inch
SHEATH O.D. = 1.090 inch
SHEATH I.D. = 1.026 inch
AIR BETWEEN SHEATH & CLAD ROD

FIG. 9 COMPONENTS USED IN MIXED LATTICE EXPERIMENTS

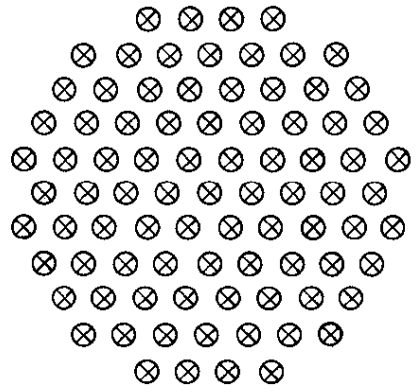

a. PDP Loading Number 1

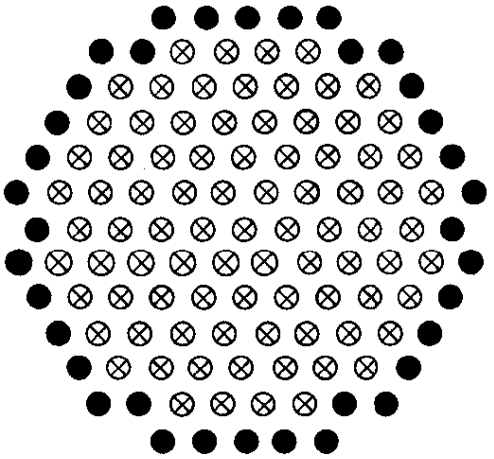

b. PDP Loading Number 2

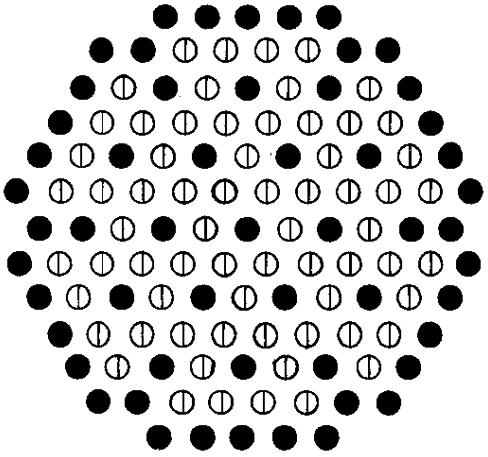

c. PDP Loading Number 3

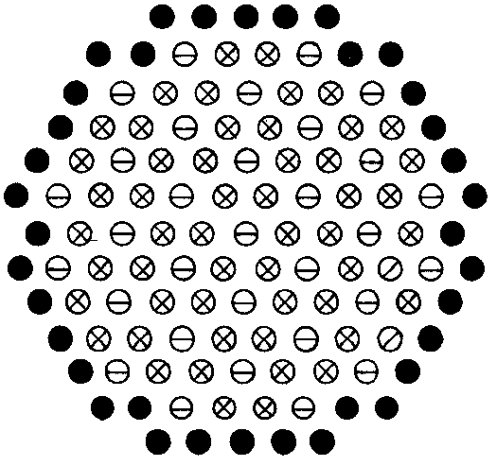

d. PDP Loading Number 4

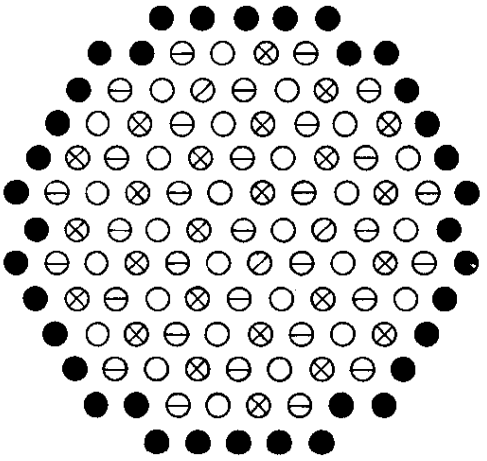

e. PDP Loading Number 5

See Figure 9

⊖	I
○	II
⊗	III
◐	IV
●	V

FIG. 10 MIXED LATTICE STUDIES

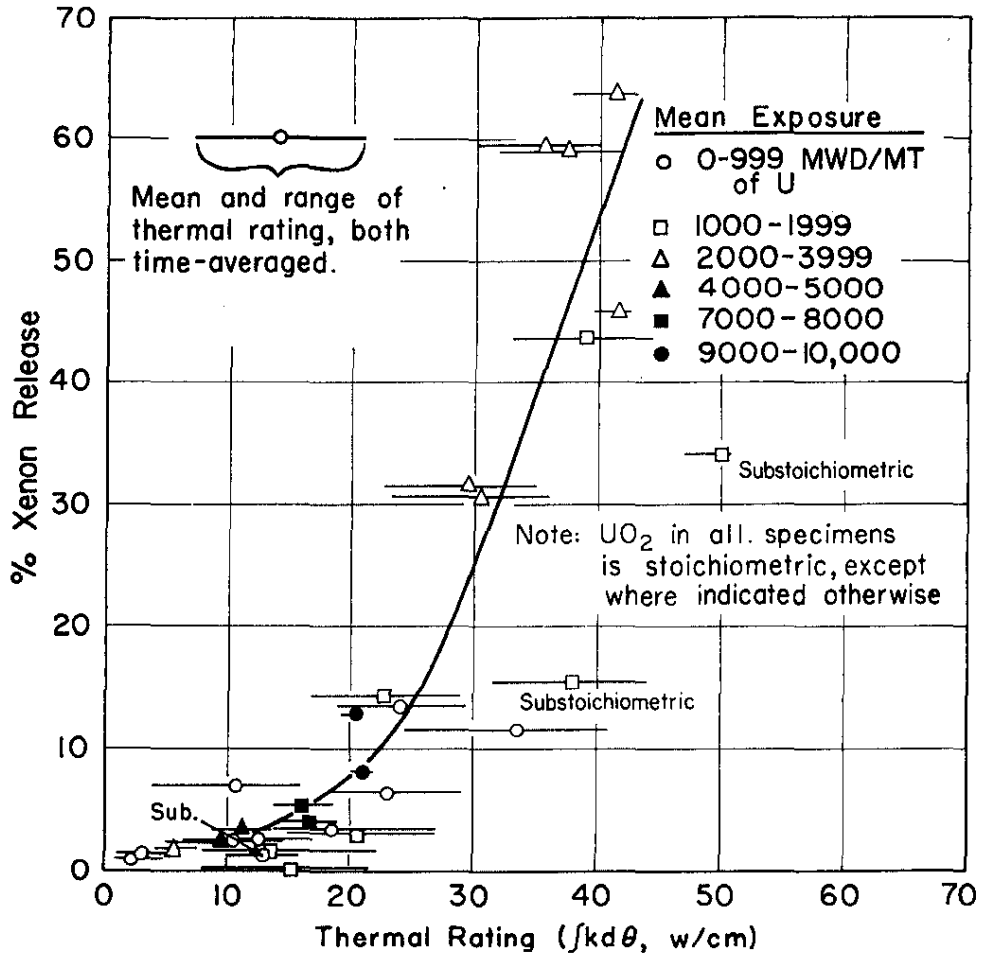

FIG. 11 EFFECT OF THERMAL RATING ON XENON RELEASE IN VIBRATED AND IN SWAGE-COMPACTED UO_2 TUBES

Neg. 59408 1.5X

FIG. 12 ANNULAR SHRINKAGE VOID IN UO_2 TUBE
Tube ZE-266A, Assembly SOT-7-2;
$\int kd\theta$ = 68 watts/cm

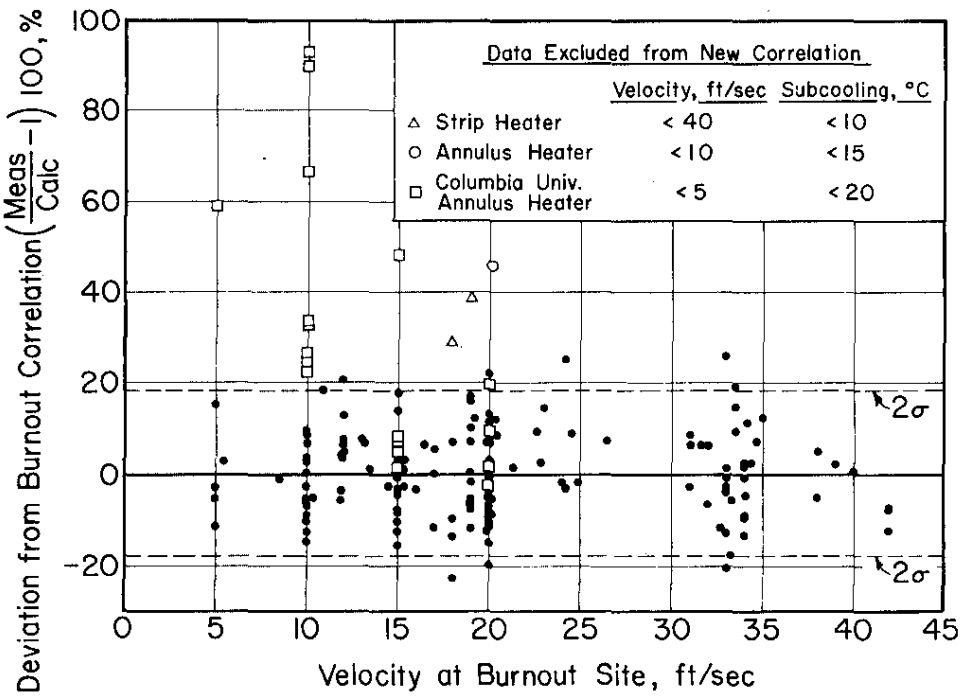

FIG. 13 DRIFT OF BURNOUT DATA WITH VELOCITY

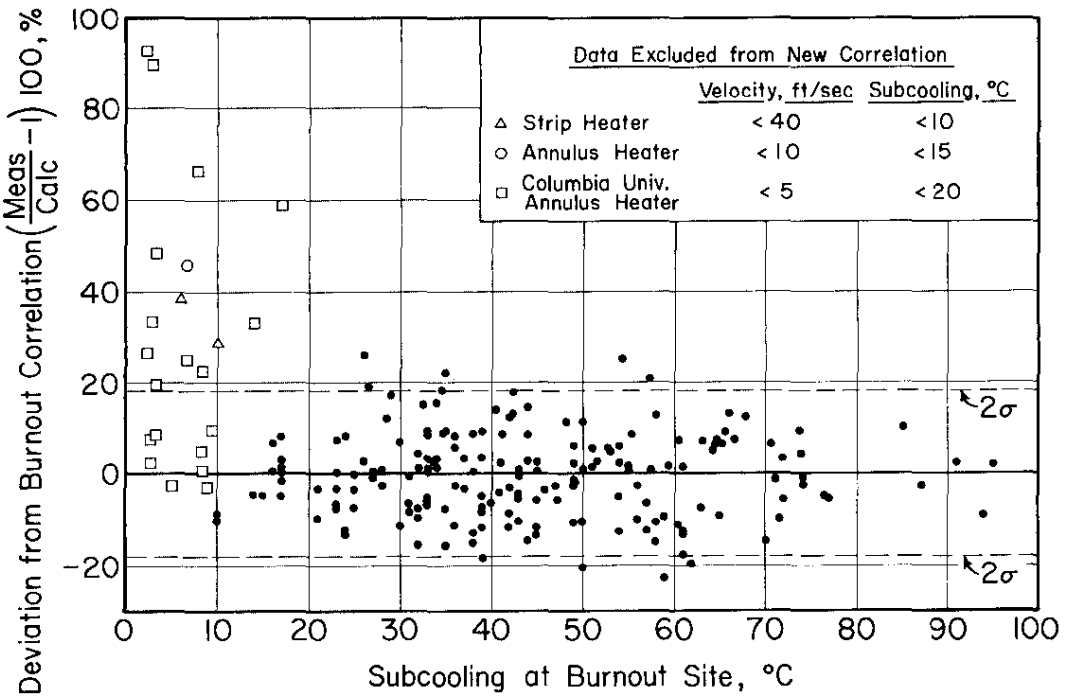

FIG. 14 DRIFT OF BURNOUT DATA WITH SUBCOOLING

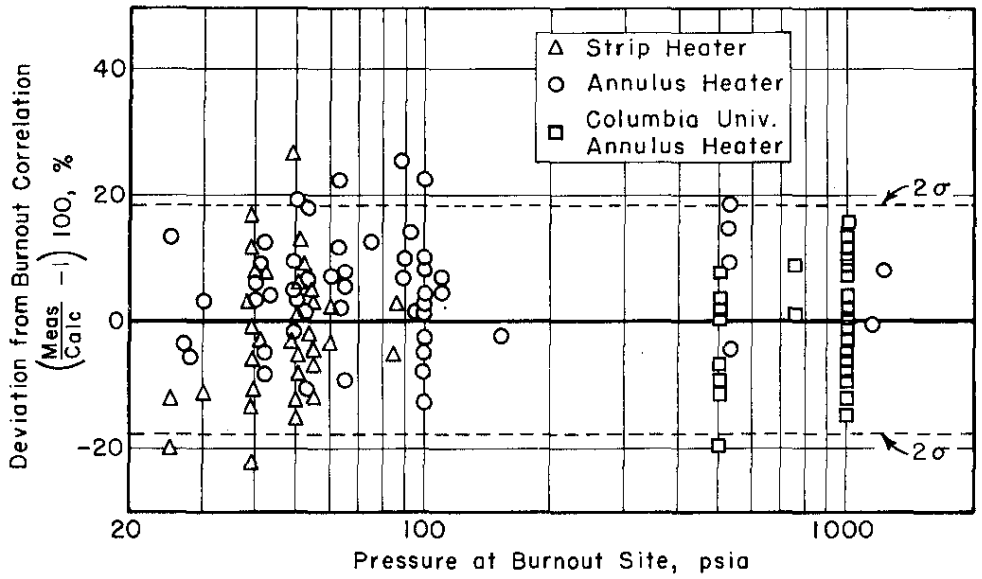

FIG. 15 DRIFT OF BURNOUT DATA WITH PRESSURE

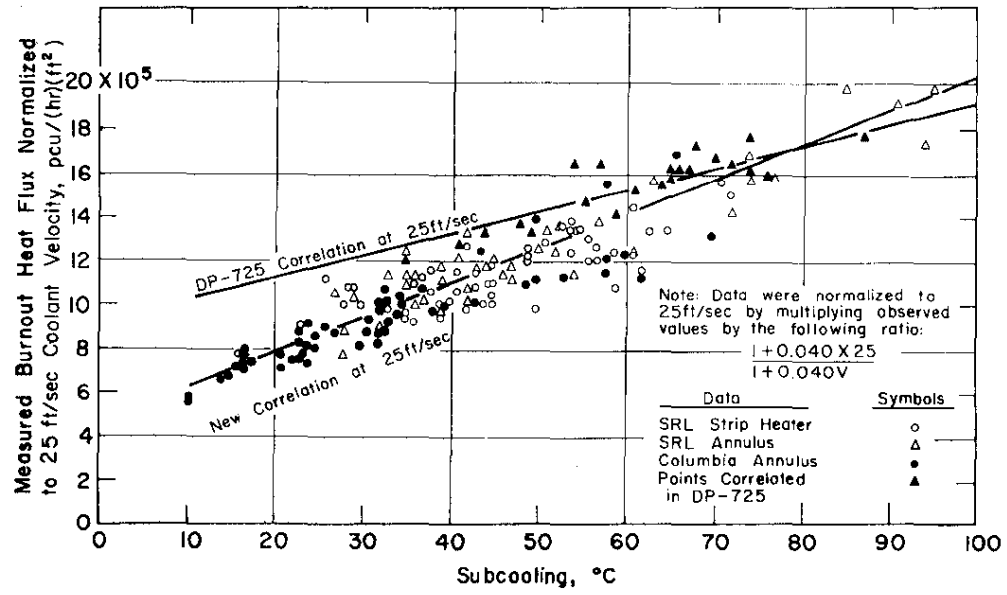

FIG. 16 COMPARISON OF BURNOUT CORRELATIONS WITH EXPERIMENTAL DATA

BIBLIOGRAPHY

1. Klahr, C. N., et al. Heterogeneous Reactor Calculation Methods. Quarterly Progress Report No. 6, Technical Research Group, USAEC Report NYO-2678 (1960).

2. Cadwell, W. R. "PDQ-3 - A Program for the Solution of the Neutron-Diffusion Equations in Two Dimensions on the IBM-704". Westinghouse Electric Corp., Bettis Atomic Power Laboratory, Pittsburgh, Pa., USAEC Report WAPD-TM-179 (1960).

3. Honeck, H. C. "THERMOS - A Thermalization Transport Theory Code for Reactor Lattice Calculations". Brookhaven National Laboratory, Upton, N. Y. USAEC Report BNL-5826 (1961).

4. Driggers, F. E. "BSQ - An IBM-704 Code to Calculate Heavy Water Lattice Parameters". Heavy Water Lattices: Second Panel Report, Technical Reports Series, No. 20, IAEA, Vienna (1963).

5. Babcock, D. F., et al. An Evaluation of Heavy-Water-Moderated Power Reactors - A Status Report as of March 1963. E. I. du Pont de Nemours & Co., Savannah River Laboratory, Aiken, S. C. USAEC Report DP-830 (1963).

6. Mirshak, S., et al. Heat Flux at Burnout. E. I. du Pont de Nemours & Co., Savannah River Laboratory, Aiken, S. C. USAEC Report DP-355 (1959).

7. Previous progress reports in this series are:

DP-232	DP-395	DP-485	DP-575	DP-665	DP-755	DP-845
DP-245	DP-405	DP-495	DP-585	DP-675	DP-765	DP-855
DP-265	DP-415	DP-505	DP-595	DP-685	DP-775	DP-865
DP-285	DP-425	DP-515	DP-605	DP-695	DP-785	DP-875
DP-295	DP-435	DP-525	DP-615	DP-705	DP-795	DP-885
DP-315	DP-445	DP-535	DP-625	DP-715	DP-805	DP-895
DP-345	DP-455	DP-545	DP-635	DP-725	DP-815	
DP-375	DP-465	DP-555	DP-645	DP-735	DP-825	
DP-385	DP-475	DP-565	DP-655	DP-745	DP-835	